5382 *Chem. Mater.* **2009,** *21,* 5382–5387
DOI:10.1021/cm901534m

CHEMISTRY OF MATERIALS
Article

Synthesis of Hierarchically Grown ZnO@NT-WS_2 Nanocomposites

Muhammad Nawaz Tahir,[†] Aswani Yella,[†] Helen Annal Therese,[†] Enrico Mugnaioli,[‡] Martin Panthöfer,[†] Hadayat Ullah Khan,[§] Wolfgang Knoll,[§] Ute Kolb,[‡] and Wolfgang Tremel*[,†]

[†]*Institut für Anorganische Chemie und Analytische Chemie der Johannes Gutenberg-Universität, Duesbergweg 10-14, D-55099 Mainz, Germany,* [‡]*Institut für Physikalische Chemie der Johannes Gutenberg-Universität, Welderweg 11, D-55099 Mainz, Germany, and* [§]*Max Planck-Institut für Polymerforschung, Ackermannweg 10, D-55128 Mainz, Germany*

Received June 4, 2009. Revised Manuscript Received September 28, 2009

A chemically specific and facile method for growth of ZnO nanorods on WS_2 nanotubes (NT-WS_2) is reported. The modification strategy is based on the chalcophilic affinity of Zn, which serves as an anchor to immobilize ZnO colloids onto the WS_2 nanotubes. The surface bound ZnO colloids have been used as a seed to grow ZnO nanorods on WS_2 nanotubes. The immobilization of ZnO colloids was monitored by UV−vis spectroscopy and photoluminescence spectroscopy whereas the growth of ZnO nanorods was characterized by scanning electron microscopy (SEM) and transmission electron microscopy (TEM).

Introduction

Tailor-made, submicrometer particles may become the building blocks of a new generation of nanostructured materials with unique physical properties. Much effort has also been devoted so far to developing hybrid materials of nanoparticles and carbon nanotubes, with the hope of discovering new properties and applications.[1,2] The properties of these nanoparticle assemblies are controlled by the composition, geometry, and the spatial arrangement of the nanoparticle building blocks. Such structures have been used for a variety of applications in catalysis, photonics, electronics, and sensing. Efforts in making such hybrid materials have been based mostly on two strategies. One is to attach certain bifunctional organic linkers to presynthesized nanoparticles and then to link the nanoparticles to the nanotubes.[3−5] This strategy uses the available synthetic know-how to control particle morphology and monodispersity; it is limited by the complexity of the surface chemistry of the nanoparticles. An alternative strategy is to grow nanoparticles directly on the nanotubes by using colloidal nanoparticle synthesis methods.[6−9] Colloidal nanoparticles may have an affinity based on their acid/base properties, functional groups, or Pearson hardness[10−12] for nanotube surfaces that allows an attachment without the aid of any linkers. This method may be adapted to produce various nanoparticle/nanotube hybrid materials, with well-controlled nanoparticle shape and quality.

As important fundamental materials, layered chalcogenide nanoparticles[13−17] and ZnO[18−23] have attracted the attention of technologists. Among the various nanoforms of ZnO, quasi-one-dimensional (1D) structures such as nanowires or nanorods have stimulated intensive interests because of their unique semiconducting and piezoelectric properties. In particular, the growth of 1D ZnO nanostructures into ordered nanoarrays has proven useful for field emission and as

*Corresponding author. Phone: +49 6131 392-5135. Fax: +49 6131 392-5605. E-mail: tremel@uni-mainz.de.

(1) Bommel, K. J. C.; Friggeri, A.; Shinkai, S. *Angew. Chem.* **2003**, *115*, 1010. Angew. Chem., Int. Ed. **2003**, *42*, 980.
(2) Mann, S. *Angew. Chem.* **2000**, *112*, 3532.Angew. Chem., Int. Ed. **2000**, *239*, 3393.
(3) Robel, I.; Bunker, B. A.; Kamat, P. V. *Adv. Mater.* **2005**, *17*, 2458.
(4) Banerjee, S.; Wong, S. S. *Nano Lett.* **2002**, *2*, 195.
(5) Sheeney-Haj-Khia, L.; Basnar, B.; Willner, I. *Angew. Chem., Int. Ed.* **2005**, *44*, 78.
(6) Olek, M.; Busgen, T.; Hilgendorff, M.; Giersig, M. *J. Phys. Chem. B* **2006**, *110*, 12901.
(7) Banerjee, S.; Wong, S. S. *Chem. Commun.* **2004**, 1866.
(8) Juarez, B. H.; Klinke, C.; Kornowski, A.; Weller, H. *Nano Lett.* **2007**, *7*, 3564.
(9) Na, Y. J.; Kim, H. S.; Park, J. *J. Phys. Chem. C* **2008**, *112*, 11218.
(10) Pearson, R. G. *J. Am. Chem. Soc.* **1963**, *85*, 3533–3539.
(11) (a) Pearson, R. G. *Chemical Hardness. Applications from Molecules to Solids*; Wiley-VCH: Weinheim, 1997. (b) Umland, F.; Wünsch, G. *Charakteristische Reaktionen Anorganischer Stoffe*, 2nd ed.; Aula Verlag: Wiesbaden, 1991.
(12) Alfarra, A.; Frackowiak, E.; Beguin, F. *Appl. Surf. Sci.* **2004**, *228*, 84–92.
(13) http://www.apnano.com/products.asp.
(14) http://www.isracast.com.
(15) Tenne, R. *Nat. Nanotechnol.* **2006**, *1*, 103.
(16) Tenne, R.; Remskar, M.; Enyashin, A.; Seifert, G. *Top. Appl. Phys.* **2008**, *111*, 631.
(17) Goldberger, J.; Fan, R.; Yang, P. *Acc. Chem. Res.* **2006**, *39*, 239.
(18) Jagadish, C.; Pearton, S. J. *Zinc Oxide Bulk, Thin Films and Nanostructures*; Elsevier: New York, 2006.
(19) Djurisic, A. B.; Leung, Y. H. *Small* **2006**, *2*, 944.
(20) Schmidt-Mende, L.; MacManus-Driscoll, J. L. *Mater. Today* **2007**, *10*, 40.
(21) Nakayama, Y.; Pauzauskie, P. J.; Radenovic, A.; Onorato, R. M.; Saykally, R. J.; Liphardt, J.; Yang, P. *Nature* **2007**, *447*, 1098.
(22) Qin, Y.; Wang, X.; Wang, Z. L. *Nature* **2008**, *451*, 809.
(23) Suh, D.; Lee, S. Y.; Hyung, J. H.; Kim, T. H.; Lee, S. K. *J. Phys. Chem. C* **2008**, *112*, 1276.

Published on Web 10/21/2009

piezo-nano-generators.[24−30] Moreover, ZnO nanomaterials are used for UV lasers,[31,32] dye sensitized solar cells,[33,34] antireflection coatings,[35,36]and photocatalysis.[37,38] The performance of ZnO in solar applications, however, is significantly lower than that reported for TiO_2. Several reports suggest dye adsorption to be a serious problem in dye-sensitized ZnO solar cells.[39,40] As tungsten sulfide quantum sheets have been reported as sensitizers for porous, nanostructured TiO_2,[41] it seems intriguing to explore the potential applications of WS_2 nanoparticles for sensitizing ZnO. For the realization of these applications, an assembling of the primary building blocks with predictable geometric shapes is required.[42,43]

Nanotubes[44,45] (NT-MQ_2) and fullerenes (IF-MQ_2)[46−48] of layered metal chalcogenides are the purely inorganic analogues of carbon fullerenes and nanotubes that exhibit analogous mechanical[49−51]and electronic properties.[52,53] Crystalline layered chalcogenides have proven suitable for efficient and stable solar energy conversion devices which might be a viable alternative to other crystalline materials for photovoltaic cells.[54]

Their physical properties[55,56] are related to their crystal structures, which contain MQ_2 slabs with metal atoms sandwiched between two inert chalcogen layers. These MQ_2 layers are stacked, with only van der Waals contacts between them. The steric shielding of the metal atoms by the chalcogen surface layers from nucleophilic attack by oxygen or organic ligands makes chalcogenide nanoparticles highly inert and notoriously difficult to functionalize. Some progress has been made by employing chalcophilic transition metals that can "wet" the sulfur surface of the chalcogenide nanoparticles while multidentate surface ligands partially block the coordination sphere of the metal thereby preventing an aggregation through cross-linking.[57−61] Here, we demonstrate a novel synthetic strategy allowing the formation of hierarchical core−shell ZnO@NT-WS_2 nanostructures by using multiwall WS_2 nanotubes as "backbone" templates.

Experimental Section

Synthesis of NT-WS_2. WS_2 nanotubes were synthesized according to the procedure reported by Therese et al.[62]

Synthesis of ZnO Colloids. A batch of ZnO colloids were synthesized by dissolving 110 mg (0.5 mmol) of Zn-$(CH_3COO)_2 \cdot 2H_2O$ in 25 mL of ethanol with sonication for 15 min at 0 °C. To the above solution was added 21 mg (0.5 mmol) of $Li(OH) \cdot H_2O$ and sonication was continued for another 15 min at the same temperature. A stable and optically transparent ZnO solution was obtained.

Immobilization of ZnO colloids on NT-WS_2. Five milligrams of NT-WS_2 was suspended in 15 mL of ethanol by sonication. To the suspension of NT-WS_2 was added 15 mL of a ZnO colloidal solution, and the suspension was stirred for 24 h. The product was collected by centrifugation and washed with ethanol three times.

Growth of ZnO Nanorods on NT-WS_2. The ZnO nanorods were grown by the method reported by Morin et al.[63] Briefly,

(24) Kitamura, K.; Tokunaga, M.; Iwane, A. H.; Yanagida, T. *Nature* **1999**, *397*, 129.
(25) Lee, C. J.; Lee, T. J.; Lyu, S. C.; Zhang, Y.; Ruh, H.; Lee, H. *J. Appl. Phys. Lett*. **2002**, *81*, 3648.
(26) Zhu, Y. W.; Zhang, H. Z.; Sun, X. C.; Feng, S. Q.; Xu, J.; Zhao, Q.; Xiang, B.; Wang, R. M.; Yu, D. P. *Appl. Phys. Lett*. **2003**, *83*, 144.
(27) Banerjee, D.; Jo, S. H.; Ren, Z. F. *Adv. Mater*. **2004**, *16*, 2028.
(28) Li, Y. B.; Bando, Y.; Golberg, D. *Appl. Phys. Lett*. **2004**, *84*, 3603.
(29) Yan, C.; Xue, D. *J. Phys. Chem. B* **2006**, *110*, 25850.
(30) Fang, X. S.; Bando, Y.; Gautam, U. K.; Ye, C. H.; Golberg, D. *J. Mater. Chem*. **2008**, *18*, 509.
(31) Bagnall, D. M.; Chen, Y. F.; Zhu, Z.; Yao, T.; Koyama, S.; Shen, M. Y.; Goto, T. *Appl. Phys. Lett*. **1997**, *70*, 2230.
(32) Huang, M. H.; Mao, S.; Feick, H.; Yan, H. Q.; Wu, Y. Y.; Kind, H.; Weber, E.; Russo, R.; Yang, P. D. *Science* **2001**, *292*, 1897.
(33) Law, M.; Greene, L. E.; Johnson, J. C.; Saykally, R.; Yang, P. D. *Nat. Mater*. **2005**, *4*, 455.
(34) Zhang, Q.; Chou, T. P.; Russo, B.; Jenekhe, S. A.; Cao, G. *Angew. Chem., Int. Ed*. **2008**, *120*, 2293. Angew. Chem., Int. Ed. **2008**, *47*, 2402.
(35) Lee, Y. J.; Ruby, D. S.; Peters, D. W.; McKenzie, B. B.; Hsu, J. W. P. *Nano Lett*. **2008**, *5*, 1501.
(36) Cheng, C.; Lei, M.; Feng, L.; Wong, T. L.; Ho, K. M.; Fung, K. K.; Loy, M. M. T.; Yu, D.; Wang, N. *ACS Nano* **2009**, *3*, 53.
(37) Pagano, J. J.; Baisaigi, T.; Steinbock, O., Jr. *Angew. Chem., Int. Ed*. **2008**, *47*, 9900.
(38) Wang, J.; Liu, P.; Fu, X.; Li, Z.; Han, W.; Wang, X. *Langmuir* **2009**, *25*, 1218.
(39) Keis, K.; Lindgren, J.; Lindquist, S.-E.; Hagfeldt, A. *Langmuir* **2000**, *16*, 4688.
(40) Bauer, C.; Boschloo, G.; Mukhtar, E.; Hagfeldt, A. *J. Phys. Chem. B* **2001**, *105*, 5585.
(41) Thomalla, M.; Tributsch, H. *J. Phys. Chem. B* **2006**, *110*, 12167.
(42) Hirsch, A. *Angew. Chem*. **2002**, *114*, 1933–1939.Angew. Chem., Int. Ed. **2002**, *41*, 1853.
(43) (a) Pacholski, C.; Kornowski, A.; Weller, H. *Angew. Chem*. **2002**, *114*, 1234. (b) Pacholski, C.; Kornowski, A.; Weller, H. *Angew. Chem., Int. Ed*. **2002**, *41*, 1188.
(44) Tenne, R.; Margulis, L.; Genut, M.; Hodes, G. *Nature* **1992**, *360*, 444.
(45) Margulis, L.; Salitra, G.; Tenne, R.; Talianker, M. *Nature* **1993**, *365*, 113.
(46) Feldman, Y.; Wasserman, E.; Srolovitz, D. J.; Tenne, R. *Science* **1995**, *267*, 222.
(47) Tenne, R.; Homyonfer, M.; Feldman, Y. *Chem. Mater*. **1998**, *10*, 3225.
(48) Tremel, W. *Angew. Chem*. **1999**, *111*, 2311.Angew. Chem., Int. Ed. **1999**, *38*, 2175.
(49) Hacohen, Y. R.; Grunbaum, E.; Tenne, R.; Sloan, J.; Hutchison, J. L. *Nature* **1998**, *365*, 336.
(50) Zhu, A. Q.; Sekine, T.; Li, Y. H.; Wang, W. X.; Fay, M. Y.; Edwards, H.; Brown, P. D.; Fleischer, N.; Tenne, R. *Adv. Mater*. **2005**, *17*, 1500.
(51) Kaplan-Ashiri, I.; Cohen, S. R.; Gartsman, K.; Rosentsveig, R.; Ivanovskaya, V.; Heine, T.; Seifert, G.; Wagner, H. D.; Tenne, R. *Proc. Natl. Acad. Sci. U.S.A*. **2006**, *103*, 523.
(52) Scheffler, L.; Rosentzveig, R.; Margolin, A.; Popovitz-Biro, R.; Seifert, G.; Cohen, S. R.; Tenne, R. *Phys. Chem. Chem. Phys*. **2002**, *4*, 2095.
(53) Nath, M.; Kar, S.; Raychaudhuri, A. K.; Rao, C. N. R. *Chem. Phys. Lett*. **2003**, *368*, 690.
(54) Tributsch, H.; Bennett, J. C. *J. Electroanal. Chem*. **1977**, *81*, 97.
(55) Hulliger, F. *Structural Chemistry of the Layer-Type Phases*; Levy, F., Ed.; Reidel, 1976.
(56) Katz, A.; Redlich, M.; Rapoport, L.; Wagner, H. D.; Tenne, R. *Tribol. Lett*. **2006**, *21*, 135.
(57) (a) Tahir, M. N.; Eberhardt, M.; Zink, N.; Therese, H. A.; Kolb, U.; Theato, P.; Tremel, W. *Angew. Chem*. **2006**, *118*, 4927. (b) Tahir, M. N.; Eberhardt, M.; Theato, P.; Faiss, S.; Janshoff, A.; Gorelik, T.; Kolb, U.; Tremel, W. *Angew. Chem., Int. Ed*. **2006**, *45*, 4809.
(58) Tahir, M. N.; Zink, N.; Eberhardt, M.; Therese, H. A.; Kolb, U.; Theato, P.; Tremel, W. *Small* **2007**, *3*, 829.
(59) (a) Tahir, M. N.; Eberhardt, M.; Theato, P.; Faiss, S.; Janshoff, A.; Gorelik, T.; Kolb, U.; Tremel, W. *Angew. Chem*. **2006**, *118*, 922. (b) Tahir, M. N.; Eberhardt, M.; Theato, P.; Faiss, S.; Janshoff, A.; Gorelik, T.; Kolb, U.; Tremel, W. *Angew. Chem., Int. Ed*. **2006**, *45*, 908.
(60) (a) Tahir, M. N.; Eberhardt, M.; Therese, H. A.; Kolb, U.; Theato, P.; Mueller, W. E. G.; Schroeder, H. C.; Tremel, W. *Angew. Chem*. **2006**, *118*, 4921. (b) Tahir, M. N.; Eberhardt, M.; Therese, H. A.; Kolb, U.; Theato, P.; Mueller, W. E. G.; Schroeder, H. C.; Tremel, W. *Angew. Chem., Int. Ed*. **2006**, *45*, 4803.
(61) Tahir, M. N.; Natalio, F.; Therese, H. A.; Yella, A.; Metz, N.; Shah, M. R.; Mugnaioli, E.; Berger, R.; Theato, P.; Schroeder, H. C.; Müller, W. E. G.; Tremel, W. *Adv. Funct. Mater*. **2009**, *19*, 285.
(62) Therese, H. A.; Li, J.; Kolb, U.; Tremel, W. *Solid State Sci*. **2005**, *7*, 67.

5 mL of a solution of HMTA (12 mM) in water was mixed with 5 mg of ZnO colloids immobilized on NT-WS_2. The suspension was stirred for 5 min. Subsequently, 5 mL of a solution of zinc nitrate (12 mM) was added. The reaction container was kept in dry oven preheated to 95 °C for 2 h. The product was collected by decantation, washed repeatedly with ethanol, and collected by centrifugation.

Conductivity Measurements. Highly doped silicon with thermally evaporated SiO_2 (200 nm) was used as a substrate. NT-WS_2 and ZnO@NT-WS_2 nanorods were dispersed on the substrate by drop-casting from a 1 mg/mL solution as illustrated in Scheme S1 (see the Supporting Information). Finally, the samples were annealed at 100 °C for 1 h. $I-V$ data were measured using a Keithley 4200 semiconductor characterization system at ambient conditions.

Physical Characterization. The products obtained were analyzed by UV−vis spectroscopy, X-ray diffraction (XRD), field emission scanning electron microscopy (FESEM), and high resolution transmission electron microscopy (HRTEM). The morphologies of the ZnO colloids, ZnO colloids immobilized on NT-WS_2, and ZnO nanorods grown on NT-WS_2 were detected by a FEI Tecnai F30 and a FEI Tecnai F20, both equipped with an FEG, scanning transmission electron microscope (STEM), and energy dispersive X-ray (EDX) detector. For TEM studies, carbon film coated copper grids containing a drop of suspension of the sample in ethanol was used. STEM images were collected by a high angular annular dark field detector. Scanning electron microscopy was carried out using a LEO 1530 field-emission scanning electron microscope, 6 kV extraction voltages. UV−vis absorption spectra were taken with an Omega-10 spectrometer (Bruins Instruments).

Results and Discussion

The modification strategy is based on the chalcophilicity of Zn^{2+} cations, which serve as an anchor to immobilize ZnO colloids on NT-WS_2. These colloids have been used in the following step as seeds to grow ZnO nanorods on NT-WS_2 as shown in Scheme 1.

The WS_2 nanotubes were prepared as described previously by the sulfidization of WO_3 nanorods obtained via hydrothermal synthesis.[62] The ZnO colloids were synthesized by basic hydrolysis of $Zn(Ac)_2 \times 2H_2O$ with LiOH in ethanol using sonication at 0 °C.[64] The ZnO nanorods were grown by wet chemistry as reported by Morin et al.[63] The immobilization of the ZnO colloids was monitored by UV−vis and photoluminescence spectroscopy, whereas the growth of ZnO nanorods was characterized by scanning electron microscopy (SEM), transmission electron microscopy (TEM), and high-resolution transmission electron microscopy (HRTEM). The as-synthesized ZnO colloids were monodisperse and well crystalline with diameters ranging from 4 to 5 nm as shown in Figure S1 (Supporting Information). They were highly soluble in ethanol and stable for several months. In order to immobilize ZnO colloids as a seed layer, the WS_2 nanotubes were dispersed in ethanol using a sonication bath while adding an ethanolic solution of the ZnO colloids. The mixture was agitated using a vortex mixer

Scheme 1. Fabrication of the ZnO@NT-WS_2 Nanocomposite[a]

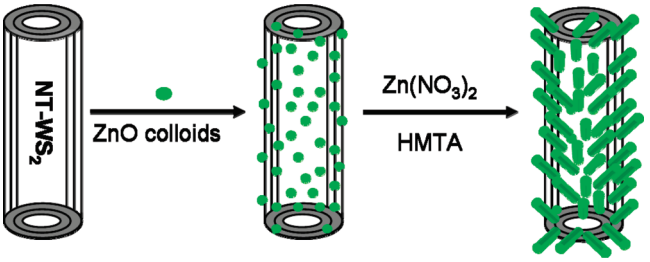

[a] In the first step, the WS_2 nanotube is functionalized with ZnO colloids (green dots). In the next step, the immobilized ZnO colloids are used as seeds to grow ZnO nanorods.

overnight. The surface binding of the ZnO colloids improved the solubility of WS_2 nanotubes in ethanol.

The immobilization of ZnO colloids on NT-WS_2 was confirmed by electron microscopy (Figure 1). The WS_2 nanotubes were uniformly coated with ZnO colloids. The HRTEM image (Figure 1b) confirms that the ZnO colloids are neither grown nor oriented on the nanotubes.

The UV−vis spectrum of the as synthesized ZnO colloids after 2 h in ethanol (Figure S2, Supporting Information) shows a characteristic absorption band edge at 368 nm (blue line). After adding 1 mg of NT-WS_2, the absorption coefficient increased while the absorption edge remained unchanged (black line). A sharp absorption band at 260 nm appeared upon the growth of ZnO nanorods (green line). The appearance of absorption bands of ZnO around 260 nm was been reported by other authors and attributed to the presence of surface defects.[65−67]

Figure 2 shows the photoluminescence spectra of ZnO colloids in ethanol at different concentrations of NT-WS_2. The outermost surface sulfur layer of NT-WS_2 serves as an anchor for immobilization of ZnO colloids. With increasing concentration of NT-WS_2, we expect more of ZnO particles to interact with the nanotubes. As a result of this interaction, there was an enhancement of photoluminescence centered at $\lambda_{max} = 545$ nm when excited at 270 nm. After carrying on the immobilization of ZnO colloids overnight, there was almost a 40% emission enhancement of ZnO, and it was red-shifted to $\lambda_{max} = 580$ nm. A plausible explanation could be that excited electrons relax from the conduction band of ZnO to the conduction band of NT-WS_2 (indirect band gap).[41,68]

ZnO nanorods were grown starting from the ZnO seeds using $Zn(NO_3)_2$ and hexamethylene tetraamine (HMTA).[63] The samples were characterized using SEM. Figure 3a shows an overview image of NT-WS_2 decorated in a brush-like fashion with ZnO nanorods. Figure 3b shows a high resolution SEM image of a single nanotube decorated with ZnO nanorods. All nanotubes are covered densely in a uniform manner with ZnO nanorods aligned perpendicular to the walls of the nanotubes.

The TEM images in Figure 4 show details of the structure and morphology of the ZnO@NT-WS_2

(63) Morin, S. A.; Amos, F.; Jin, S. *J. Am. Chem. Soc.* **2007**, *129*, 13776.
(64) Vietmeyer, F.; Seger, B.; Kamat, P. V. *Adv. Mater.* **2007**, *19*, 2935.
(65) Li, C.; Yu, Z.; Fang, S.; Wang, H.; Gui, H.; Xu, J.; Chen, R. *J. Alloys Compd.* **2009**, *475*, 718.
(66) Paul, W. L. *Phys. Rev.* **1961**, *123*, 1226.
(67) Mo, C. M.; Zhang, L.; Yuan, Z. *Nanostruct. Mater.* **1995**, *5*, 95.
(68) Grätzel, M. *Nature* **2001**, *414*, 338–344.

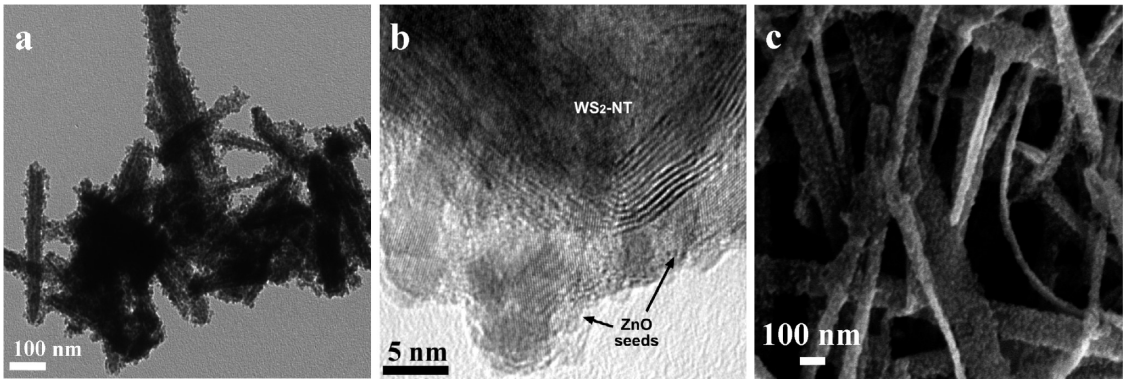

Figure 1. ZnO colloids immobilized on WS_2 nanotubes: (a) overview TEM, (b) HRTEM, and (c) overview SEM.

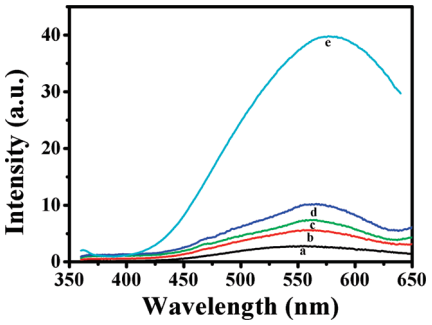

Figure 2. Emission spectra of ZnO colloids (λ_{ex} = 277 nm) in ethanol with increasing concentrations of NT-WS_2: (a) 0, (b) 150, (c) 300, (d) 450 μg. Line e shows the emission spectra of ZnO colloids after overnight stirring with 450 μg of NT-WS_2.

assembly. The overview TEM images (Figure 4a and b) reveal a homogeneous growth of ZnO nanorods on NT-WS_2. The length of the ZnO nanorods varies from 100 nm to a few hundred nanometers on different nanotubes, but it is worth mentioning that on the same nanotube the length and diameter of the nanorods are quite uniform. The average diameter of the nanorods is 40−50 nm (Figure 4c).

The corresponding magnified STEM image of Figure 4a is shown as Figure 5a. The nanotubes can be recognized within all the composites as they show a darker contrast than the ZnO nanorods (in dark field imaging). Principally, NT-WS_2 should look bright, but the contrast of nanotubes in EDX is inverted due to the saturation of the detector. EDX analysis confirms that NT-WS_2 are the core template and the ZnO nanorods are hierarchically assembled on them (Figure 5b and c). The line scan profile in Figure S3 (Supporting Information) also proves the presence of NT-WS_2 in the middle of the composites.

HRTEM and NED (nano electron diffraction) observations on selected nanorods revealed single crystal wurtzite with clear lattice fringes. (Figure 4d). The enlarged images shows the lattice fringes with *d*-spacings of d_{001} = 0.52 nm and d_{100} = 0.28 nm as expected for hexagonal ZnO. The growth direction of the nanorods is [001]. Due to the fact that ZnO nanorods are uniformly and densely packed on the WS_2 nanotubes, it was difficult to focus on the interface. However, the growth of the ZnO nanorods seems seed mediated as evidenced by the HRTEM image shown in Figure S4 (Supporting Information). As a control, the growth of ZnO in the absence (of surface bound) ZnO seed colloids resulted in the formation of a surface film and no formation of ZnO nanorods. The corresponding TEM data are provided in Figure S5 (Supporting Information).

The orientation and the polymorph selection of the grown ZnO nanorods on NT-WS_2 were confirmed by the XRD investigation. Figure S6 (Supporting Information) shows the XRD patterns of the as-synthesized ZnO colloids and the ZnO nanorods grown on NT-WS_2. For the as-synthesized ZnO colloids, the reflections are broader, and the (002) reflection appears as a shoulder of (101), but after the growth of ZnO nanorods, the (002) reflection appears as a sharp shoulder overlapped by the (101) reflection of NT-WS_2 which may indicate the formation of rods along the *c*-axis.[69]

Figure 6 shows a current vs voltage ($I-V$) plots of an SiO_2 coated substrate surface (circles), NT-WS_2 (square), and a ZnO@NT-WS_2 nanocomposite (triangles). The red lines on NT-WS_2 (square) and ZnO@NT-WS_2 nanocomposite (triangles) plots show the tunneling model fitting. The $I-V$ plots show a cubic dependence of the current on the applied electric field as known for direct tunneling between junctions,[70]

$$I \sim \beta(V + \theta V^3) \quad (1)$$

In the case of pure NT-WS_2, the Au electrode shows ohmic contact, whereas it is Schottky-type for ZnO@NT-WS_2 nanocomposites as shown in the inset of Figure 6. However, the current behavior of ZnO@NT-WS_2 nanocomposites at high voltage is dominated by barrier limited tunneling conduction across the NT-WS_2/ZnO nanocomposite contacts as described in eq 1 above. The coefficient of this cubic dependence (θ) increases by nearly one order in magnitude for the case of the ZnO@NT-WS_2 nanocomposite film. This could arise from a lowering of the barrier height for the tunneling across the individual nanocomposites, because θ has

(69) Greene, L. E.; Law, M.; Goldberger, J.; Kim, F.; Johnson, J. C.; Zhang, Y.; Saykally, R. J.; Yang, P. *Angew. Chem., Int. Ed.* **2003**, *42*, 3031.
(70) Simmons, J. G. *J. Appl. Phys.* **1963**, *34*, 238.

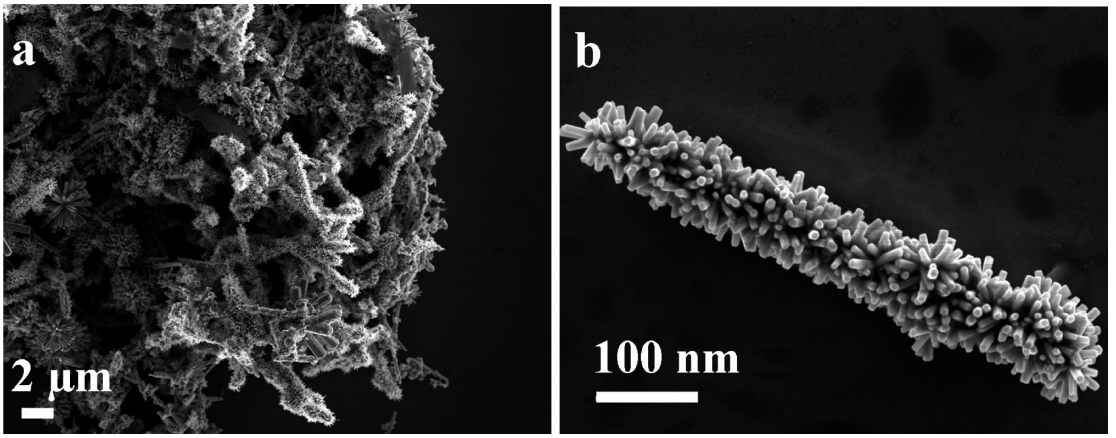

Figure 3. (a) Overview SEM image demonstrating the growth of ZnO nanorods. (b) High resolution SEM image showing the morphology of a ZnO@ NT-WS_2 hybrid nanorod.

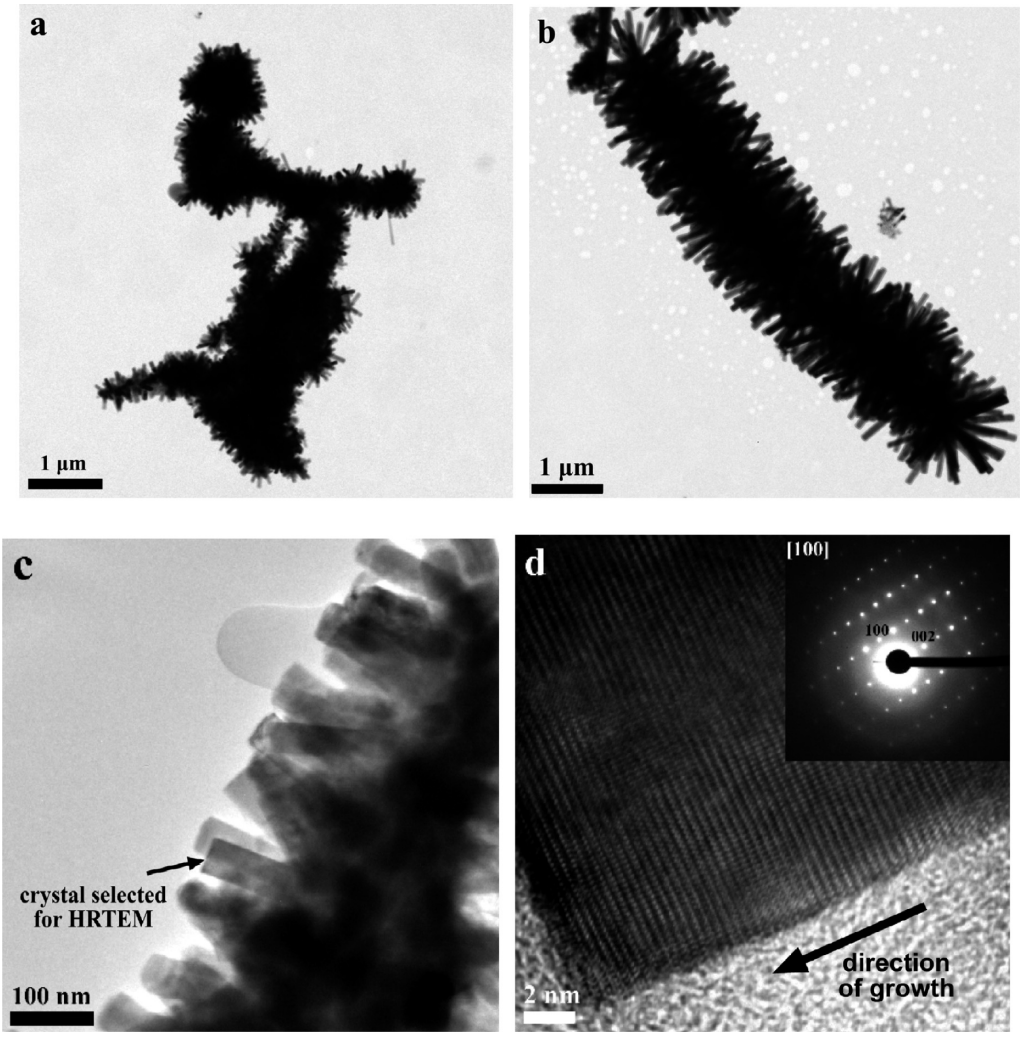

Figure 4. (a−c) Overview TEM images of ZnO@NT-WS_2 composites synthesized using ZnO colloids as seed. (d) High resolution TEM image and electron diffraction of a grown ZnO nanorod.

an inverse dependence on the tunneling barrier height. The current within an individual nanocomposite is known to be thermally activated from previous investigations.[71]

(71) Park, J. Y.; Kim, H. J.; Kim, S. S. *Nanotechnology* **2006**, *17*, 1255.

Summary and Conclusions

In summary, the selective anchoring of ZnO colloids enables a hierarchical growth of dense arrays of ZnO nanorods on WS_2 chalcogenide nanotubes. Due to the chalcophilicity of Zn, the ZnO colloidal seed particles adhere very well to the chalcogen interface, i.e. the use of

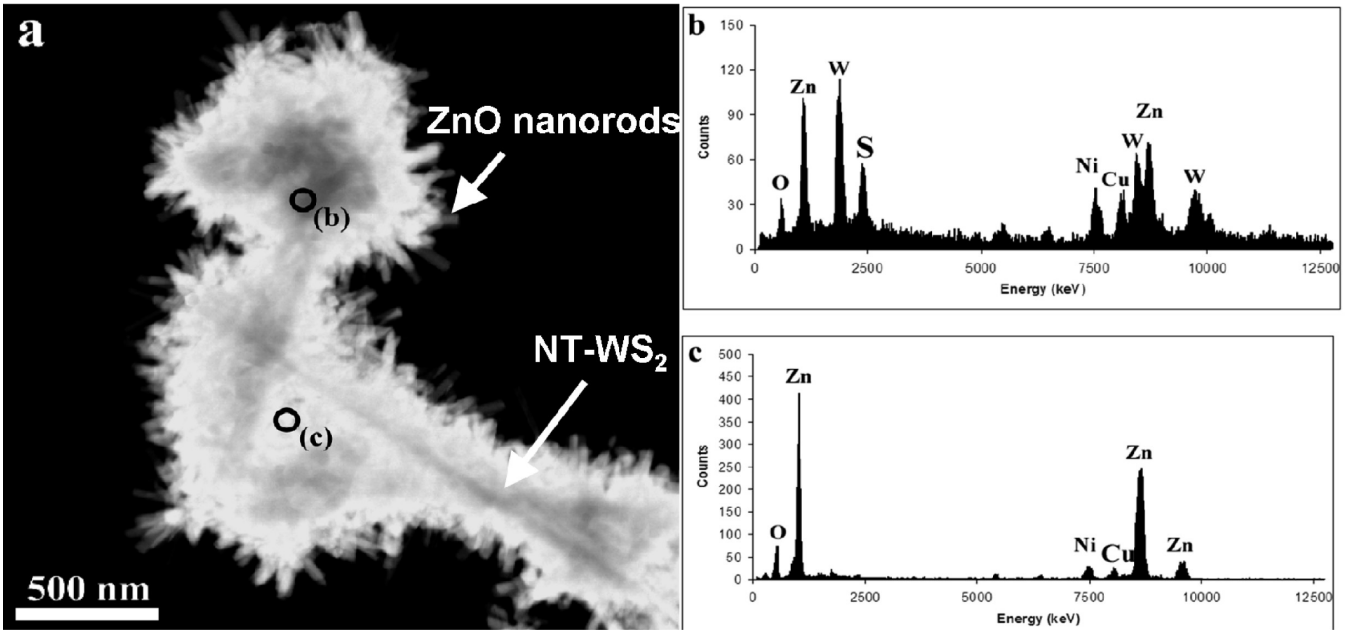

Figure 5. STEM image showing the contrast of NT-WS_2 with respect to hierarchically grown ZnO nanorods and the corresponding EDX spectra recorded from different positions of the aggregate.

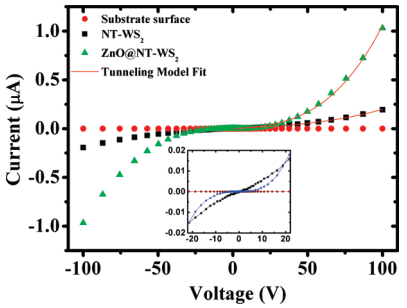

Figure 6. $I-V$ curves of the SiO_2 coated substrate surface (circles), NT-WS_2 (squares), and ZnO@NT-WS_2 nanocomposites (triangles) as measured in air at room temperature. The inset shows magnified $I-V$ curves at low voltage.

small, homogeneous ZnO nanocrystals as a seed layer helps produce a full coverage of ZnO nanorods on WS_2 nanotubes. The similarity of the lattice parameters of WS_2 and ZnO (lattice mismatch ≈3% at the interface) may play an important role in the "wetting" of the ZnO colloids, although it does not determine the growth direction of the secondary nanorod arrays. The nanorods are well-oriented and are in intimate contact with the nanotubes. The photoluminescence studies show that the obtained vertical ZnO nanorod arrays exhibit strong UV luminescence with a near-band-edge energy and the enhancement of PL due to electronic interaction between ZnO and the layered metal chalcogenide. The nanorod defined arrays of this sort may be useful for sensors and field emission or as light emitting devices. Moreover, ZnO@NT-WS_2 nanocomposites shows the enhanced electrical properties, hold a good potential to be used in future optoelectronic devices such as photoelectrochemical cells, light emitting diodes, and field effect transistors.[72,73] The "self-assembled" hybrid architecture can incorporate various different selective nanoparticle−substrate interactions based on well-known surface chemistries. Therefore, it should be useful for fabricating a range of oxide, nitride, or halide hybrid nanostructures. This growth technique offers benefits for low-cost, low-waste manufacturing, and such methods are becoming increasingly important in the development of green nanofabrication strategies. We are currently investigating whether this approach enables tuning of the nanorod diameter and spacing through control of nanoparticle core diameter, ligand shell length, and growth temperature.

Acknowledgment. This work was supported by the Deutsche Forschungsgemeinschaft (DFG) through the SPP 1165, the Materials Science Center (MWFZ), and the Electron Microscopy Center (EZMZ). We thank Dr. I. Lieberwirth and Mr. G. Glasser from the Max Plank-Institut für Polymerforschung, Mainz, for TEM and SEM support.

Supporting Information Available: Figures S1−S6 and Scheme S1. This material is available free of charge via the Internet at http://pubs.acs.org.

(72) Datta, A.; Panda, S. K.; Chaudhuri, S. *J. Phys. Chem. C* **2007**, *111*, 17260.
(73) Sun, B.; Sirringhaus, H. *J. Am. Chem. Soc.* **2006**, *128*, 16231.